Monthly Notices
of the
ROYAL ASTRONOMICAL SOCIETY

Mon. Not. R. Astron. Soc. **421,** 780–788 (2012) doi:10.1111/j.1365-2966.2011.20352.x

Outward migration of a giant planet with a gravitationally unstable gap edge

Min-Kai Lin[1,2]★ and John C. B. Papaloizou[1]★

[1]*Department of Applied Mathematics and Theoretical Physics, University of Cambridge, Centre for Mathematical Sciences, Wilberforce Road, Cambridge CB3 0WA*
[2]*Canadian Institute for Theoretical Astrophysics, 60 St. George Street, Toronto, ON M5S 3H8, Canada*

Accepted 2011 December 7. Received 2011 November 16; in original form 2011 September 27

ABSTRACT

We present numerical simulations of disc–planet interactions where the planet opens a gravitationally unstable gap in an otherwise gravitationally stable disc. In our disc models, where the outer gap edge can be unstable to global spiral modes, we find that as we increase the surface density scale the gap becomes more unstable and the planet migrates outwards more rapidly. We show that the positive torque is provided by material brought into the planet's co-orbital region by the spiral arms. This material is expected to execute horseshoe turns upon approaching the planet and hence torque it. Our results suggest that standard type II migration, applicable to giant planets in non-self-gravitating viscous discs, is likely to be significantly modified in massive discs when gravitational instabilities associated with the gap occur.

Key words: hydrodynamics – methods: numerical – protoplanetary discs – planetary systems.

1 INTRODUCTION

One of the common approximations in studies of disc–planet interactions is to adopt a non-self-gravitating disc. Thus, despite over three decades since the work of Goldreich & Tremaine (1979, 1980), only a relatively small number of studies have adopted self-gravitating disc models (Nelson & Benz 2003a,b; Pierens & Huré 2005; Baruteau & Masset 2008; Zhang et al. 2008; Ayliffe & Bate 2010). Disc gravity was included in these works in order to obtain a self-consistent treatment of planetary migration. The discs remain gravitationally stable.

Recently, Baruteau, Meru & Paardekooper (2011) and Michael, Durisen & Boley (2011) performed numerical simulations of planetary migration in gravitationally unstable discs. These studies were motivated by the need to understand the fate of giant planets formed by disc instability (Durisen et al. 2007). Consequently, these authors consider massive discs which are gravitationally unstable without the presence of a planet because the surface density is high enough and the disc is sufficiently cool (see Toomre 1964).

However, there are other types of gravitational instabilities in discs. Of particular relevance to disc–planet interactions is gravitational instability associated with internal disc edges and grooves (Papaloizou & Savonije 1991; Sellwood & Kahn 1991), as it is known that giant planets open annular gaps in discs (Lin & Papaloizou 1986).

Meschiari & Laughlin (2008) suggested planetary gaps may become gravitationally unstable by analysing the stability of a prescribed disc profile. Instability was explicitly confirmed by Lin & Papaloizou (2011a) via linear and non-linear calculations for gaps self-consistently opened by a planet. Lin & Papaloizou called these instabilities *edge modes* since they are associated with gap edges.

In this study we explore the consequence of edge modes on planetary migration using hydrodynamic simulations. We consider the specific configuration of a giant planet residing in a gap with unstable gap edges. Our specific aim is to understand how edge modes can modify the standard picture of planetary migration expected for giant planets. We therefore focus on a small set of simulations rather than a full parameter survey.

This paper is organized as follows. We describe our disc–planet models and numerical methods in Section 2. In Section 3 we discuss the expected stability properties of planetary gaps formed in our discs. We present migration results in Section 4. We find that the planet migrates *outwards* as the gap edge becomes increasingly unstable. We analyse a case in Section 5 to identify the required source of positive torque and explain how this can be attributed to edge modes. We conclude in Section 6 with a discussion of implications and limitations of our results.

2 MODEL SETUP

We consider a two-dimensional self-gravitating protoplanetary disc of mass $M_{\rm d}$ orbiting a central star of mass M_*. We adopt polar coordinates $\boldsymbol{r} = (r, \phi)$ centred on the star and a non-rotating reference frame. The governing hydrodynamic equations are given in Lin & Papaloizou (2011a). Units are such that $M_* = G = 1$, where G is the gravitational constant.

★E-mail: mklin924@cita.utoronto.ca (M-KL); j.c.b.papaloizou@damtp.cam.ac.uk (JCBP)

The disc occupies $r \in [r_i, r_o] = [1, 25]$ and its surface density Σ is initialized to

$$\Sigma(r) = \Sigma_0 r^{-3/2} \left[1 - \sqrt{\frac{r_i}{r + H(r_i)}}\right], \quad (1)$$

where $H(r)$ is the disc semi-thickness defined below, and the surface density scale Σ_0 is chosen by specifying the Keplerian Toomre Q parameter at the outer boundary

$$Q_o = \left.\frac{c_{iso}\Omega_k}{\pi G \Sigma}\right|_{r_o}, \quad (2)$$

where

$$\Omega_k = \sqrt{\frac{GM_*}{r^3}} \quad (3)$$

is the Keplerian orbital frequency, and

$$c_{iso} = H\Omega_k \quad (4)$$

is the sound-speed profile for a locally isothermal disc. We set $H(r) = hr$ and fix the aspect-ratio $h = 0.05$. The disc is also characterized by a uniform kinematic viscosity $\nu = 10^{-5}$ in dimensionless units. The initial azimuthal velocity v_ϕ is set from centrifugal balance with stellar gravity, disc gravity and pressure. The initial radial velocity is set to $v_r = 3\nu/2r$.

We introduce a planet of fixed mass $M_p = 2 \times 10^{-3} M_*$ on a circular orbit at $r = 10 = r_p(t = 0)$. This value of M_p corresponds to 2 Jupiter masses if $M_* = M_\odot$, which opens a deep gap leading to type II migration in a typical non-self-gravitating viscous disc (Lin & Papaloizou 1986), provided no instabilities develop. In this standard picture, migration follows the viscous evolution of the gap.

2.1 Equation of state

The equation of state (EOS) is locally isothermal, so the vertically integrated pressure is $p = c_s^2 \Sigma$. Before introducing the planet, we set $c_s = c_{iso}$. When a planet is present, the sound speed c_s is prescribed as

$$c_s = \frac{hr h_p d_p}{[(hr)^{7/2} + (h_p d_p)^{7/2}]^{2/7}} \sqrt{\Omega_k^2 + \Omega_{kp}^2}, \quad (5)$$

where $\Omega_{kp}^2 = GM_p/d_p^3$, $d_p = \sqrt{|\boldsymbol{r} - \boldsymbol{r}_p|^2 + \epsilon_p^2}$ is the softened distance to the planet, $\boldsymbol{r}_p$ being its vector position and ϵ_p is the softening length. The parameter h_p controls the increase in sound speed near the planet, relative to the c_{iso} profile above, and is fixed to $h_p = 0.5$. The increase in sound speed is $c_s/c_{iso} = 1.54, 1.18$ at r_h and $2r_h$ away from the planet, respectively, where $r_h = (M_p/3M_*)^{1/3} r_p$ is the Hill radius. Far away from the planet, the sound speed becomes close to c_{iso}.

This EOS was proposed by Pepliński, Artymowicz & Mellema (2008a) in a series of numerical simulations of type III migration in non-self-gravitating discs. The c_{iso} profile, commonly used in disc–planet simulations, leads to mass accumulation near the planet and could lead to spurious torques from within the planet's Hill radius. In a self-gravitating disc, it also causes the effective planetary mass M_p', which is M_p plus disc material gravitationally bound to the planet (Crida et al. 2009), to increase with the disc surface density scale (Lin & Papaloizou 2011b).

Equation (5) increases the temperature near $\boldsymbol{r}_p$, thereby reducing the mass accumulation and effects above. Physically, disc material can be expected to heat up as it falls into the planet potential and provide a pressure buffer limiting further mass accumulation. The use of equation (5) in the present work is a simplified prescription for accounting for this. However, the gaps opened in a disc with $c_s = c_{iso}$ and with equation (5) are similar. The gap widths are identical and the gap depth is <5 per cent deeper in the case with $c_s = c_{iso}$.

2.2 Numerical methods

The hydrodynamic equations are integrated using the FARGO code (Masset 2000a,b; Baruteau & Masset 2008). The disc is divided into $N_r \times N_\phi = 1024 \times 2048$ zones in radius and azimuth, spaced logarithmically and uniformly, respectively. The resolution is approximately 16 cells per H (or 28 cells per r_h). The cells are nearly square ($\Delta r/r\Delta\phi = 1.02$). An open boundary condition is applied at r_i and a non-reflecting boundary condition at r_o (as used by Zhang et al. 2008, see also Godon 1996). Self-gravity is solved via a 2D Poisson integral, in which a softening length $\epsilon_g = 0.3H$ is set to prevent divergence and approximately account for the disc's vertical thickness (Baruteau & Masset 2008).

The planet is introduced with zero mass at time $t = 20P_0$, where $P_0 = 2\pi/\Omega_k(r_p(t = 0))$ is the Keplerian period at the planet's initial orbital radius. Its mass is then increased smoothly over $10P_0$ to its final value M_p. The planet is then allowed to respond to disc gravitational forces for $t > 30P_0$. A standard fifth-order Runge–Kutta scheme is used to integrate its equation of motion. The softening length for the planet potential is $\epsilon_p = 0.6H$.

3 GAP STABILITY

We first consider gap profiles in disc models with $Q_0 = 1.5, 1.7, 2.0$ to assess their stability. These correspond to Keplerian Toomre values at the planet's initial radius of $Q_p = 2.77, 3.14, 3.70$ and total disc masses of $M_d/M_* = 0.080, 0.071, 0.060$, respectively. The discs are gravitationally stable to axisymmetric perturbations. For smooth radial profiles, they are also expected to be gravitationally stable to non-axisymmetric perturbations near r_p because $Q_p > 1.5$.

The fundamental quantity for stability discussion in a structured barotropic disc is the vortensity[1] (e.g. Papaloizou & Lin 1989; Lovelace et al. 1999)

$$\eta = \frac{\kappa^2}{2\Omega\Sigma}, \quad (6)$$

where $\kappa^2 = r^{-3}\mathrm{d}(r^4\Omega^2)/\mathrm{d}r$ is square of the epicycle frequency and $\Omega = v_\phi/r$ is the angular velocity. For gaps opened by a giant planet, the vortensity profile closely follows the Toomre Q profile when the latter is calculated with κ instead of Ω_k. Specifically, local extrema in η and Q occur approximately at the same radii (Lin & Papaloizou 2011a).

Lin & Papaloizou (2011a) have shown that planetary gaps in massive discs are unstable to global edge modes associated with $\max(\eta)$ or $\max(Q)$. For the adopted disc models, the background Keplerian Toomre parameter decreases with r, i.e. the disc is more self-gravitating at larger radii. Thus edge modes are mostly associated with the outer disc ($r > r_p$), as found by Lin & Papaloizou (2011a).

Fig. 1 compares the relative surface density perturbation and the Toomre Q parameter for gaps in the above disc models. We expect edge modes to have corotation radius r_c at a vortensity maximum, or about $2r_h$ from the planet. This corresponds to a local minimum in

[1] Strictly speaking, our discs are not barotropic. However, the instabilities of interest are associated with an internal structure with characteristic thickness $H \ll r$, but the sound speed varies on a global scale and can be approximated as constant, i.e. strictly isothermal and hence barotropic.

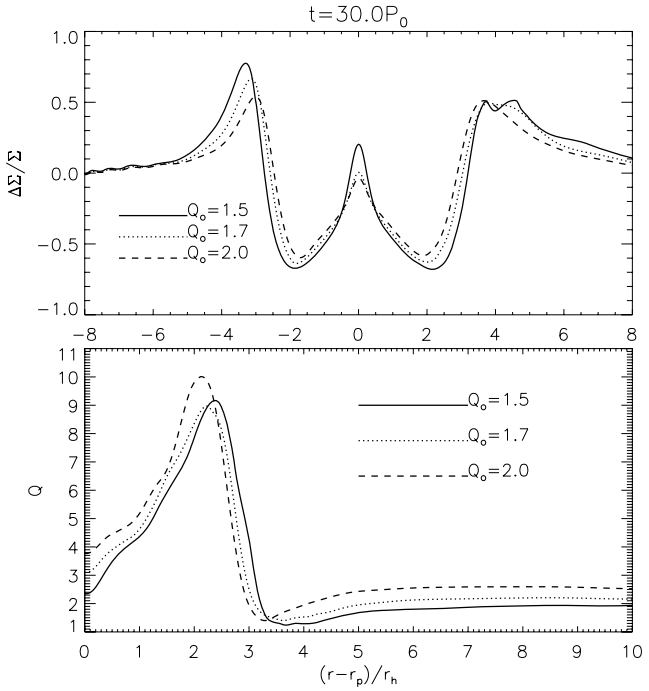

Figure 1. One-dimensional profiles of the azimuthally averaged relative surface density perturbation (top) and Toomre Q in the outer disc (bottom). Edge modes require a sufficiently peaked max(Q). In our disc models, instability is most prominent in $r > r_{\rm p}$.

relative surface density perturbation just inside the gap. Assuming the co-orbital region of a giant planet is such that $|r - r_{\rm p}| \lesssim 2.5 r_{\rm h}$ (Artymowicz 2004; Paardekooper & Papaloizou 2009), $r_{\rm c}$ is just within the outer gap edge. This suggests the development of edge modes could bring overdensities into the co-orbital region of the planet.

Edge modes also require coupling to the outer smooth disc via self-gravity, which is easier with lower $Q_{\rm o}$. The profiles here indicate edge modes will develop more readily with increasing disc mass and therefore have more significant effect on migration as $Q_{\rm o}$ is lowered.

Differences in gap profiles are also attributable to different effective planet masses, $M_{\rm p}'$. Without carefully choosing $M_{\rm p}$ and the EOS parameter $h_{\rm p}$, it is not possible to have exactly the same $M_{\rm p}'$ in discs of varying Σ_0. $M_{\rm p}'$ typically increases with increasing Σ_0, which promotes instability because gap edges become sharper. However, increasing surface density generally favours gravitational instability. Thus, planetary gaps in discs with decreasing $Q_{\rm o}$ are increasingly unstable, though perhaps more so than if $M_{\rm p}'$ is held fixed.

Giant planets can also induce fragmentation in self-gravitating discs, a phenomenon previously reported in smoothed particle hydrodynamic calculations (Armitage & Hansen 1999; Lufkin et al. 2004). Indeed, for a test run with $Q_{\rm o} = 1.3$, we found the planetary wake, as well as the disc, fragments into clumps and no annular gap can be identified. In this case migration is expected to be strongly affected by clumps, instead of large-scale spiral arms which we will focus on below.

4 MIGRATION AND DISC STRUCTURE

The above discussion suggests that edge modes could lead to non-axisymmetric disturbances inside the gap. Torques may then originate from within the planet's co-orbital region. Because $r_{\rm c}$ is expected near the outer edge of the co-orbital region, edge

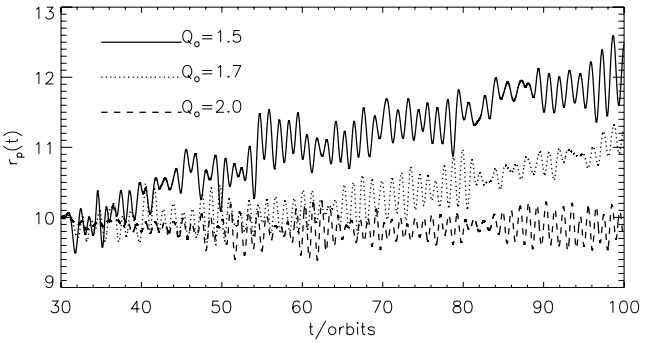

Figure 2. Migration of a giant planet in massive discs. The $Q_{\rm o} = 1.5$ and $Q_{\rm o} = 1.7$ models develop edge modes throughout, whereas the $Q_{\rm o} = 2.0$ model first develops vortex modes.

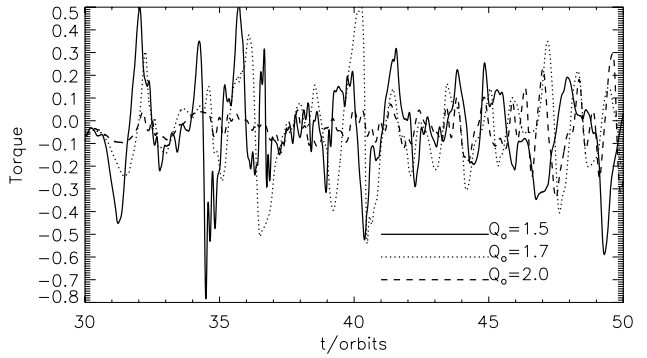

Figure 3. Instantaneous disc-on-planet torques. We have made this plot more comprehensible by multiplying the torques by a factor $f = 1 - \exp(-|\boldsymbol{r} - \boldsymbol{r}_{\rm p}|^2/r_{\rm h}^2)$. This reduces local contributions from the Hill sphere but does not affect the important feature – rapid oscillatory torques – or their behaviour as a function of $Q_{\rm o}$. Despite tapering, instabilities still have significant impact on disc–planet torques.

mode overdensities may undergo horseshoe turns upon approaching the planet. Furthermore, fluid elements just inside the separatrix will traverse close to the planet when executing U-turns, and this may provide significant torques. With this in mind, in this section we aim to identify the correlation between migration and gap evolution.

Fig. 2 shows the instantaneous orbital radius of the planet in the above disc models. Migration is non-monotonic and can be inwards or outwards on short time-scales ($\sim P_0$). However, with increasing disc mass, outward migration is favoured on time-scales of a few tens of orbits. For $Q_{\rm o} = 1.5$, $r_{\rm p}$ increases by 20 per cent in only $70P_0$. This is distinct from standard type II migration, which is inwards and occurs on much longer, viscous time-scales [$t_\nu = r^2/\nu = O(10^4 P_0)$ for our choice of ν].

Fig. 3 shows the instantaneous disc-on-planet torques during the first $20P_0$ after releasing the planet. Instabilities develop within this time frame and cause the torque to be positive or negative at a given instant. Up to about $t = 40P_0$, the torques for $Q_{\rm o} = 1.5$ and $Q_{\rm o} = 1.7$ both show large and rapid oscillations in comparison to the $Q_{\rm o} = 2.0$ case. We shall see that this is related to edge modes developing for $Q_{\rm o} = 1.5, 1.7$ but not for $Q_{\rm o} = 2.0$.

4.1 Disruption of the outer gap edge

The behaviour of $r_{\rm p}(t)$ correlates with gap structure, particularly the outer gap edge. Fig. 4 shows the relative surface density perturbation

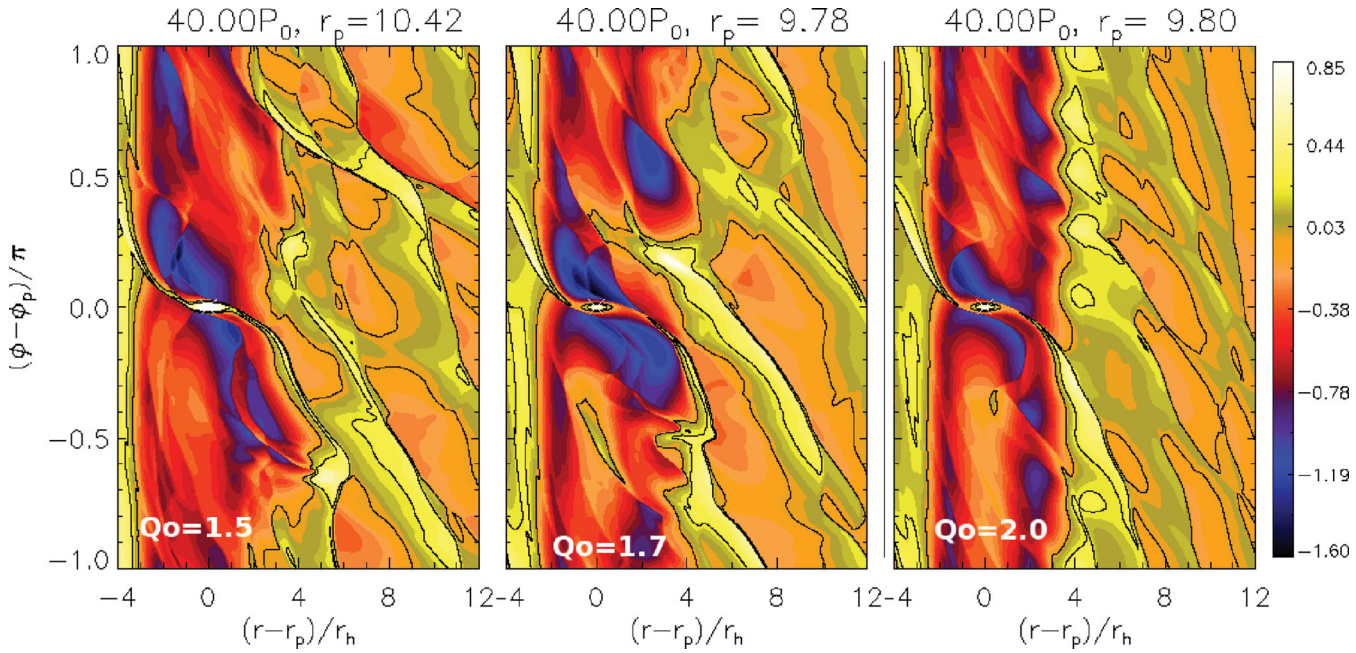

Figure 4. Logarithmic relative surface density perturbation, $\log[\Sigma/\Sigma(t=0)]$, showing gap instability as a function of Q_o. As Q_o is lowered, the outer gap edge becomes more unstable. This correlates with an increasing tendency for outward migration.

when instabilities first develop. The least massive disc with $Q_o = 2.0$ develops vortices rather than global edge modes (cf. $Q_o = 1.7$). This can be expected since edge modes require sufficiently strong self-gravity (Lin & Papaloizou 2011a).

In weakly or non-self-gravitating structured discs, unstable modes are associated with local vortensity minima (Lin & Papaloizou 2011b) and lead to vortex formation. The basic state (Fig. 1) shows that local min(Q), hence min(η), is located exterior to max(Q), and is most pronounced for $Q_o = 2.0$. We did observe spiral arms to develop in $Q_o = 2.0$ later on, but these probably resulted from the vortices perturbing the disc, rather than the linear edge mode instability. The important point with $Q_o = 2.0$ is that instability leaves the outer gap edge intact and identifiable, unlike for more massive discs.

In Fig. 4, the $Q_o = 1.7$ case develops an $m = 2$–3 edge mode. Protrusion of the spiral arms into the gap makes the outer gap edge less well-defined. The surface density in the gap is on average higher in $\phi > \phi_p$ than in $\phi < \phi_p$. The edge mode spiral inside the gap and just upstream of the planet could provide a significant positive torque as the spiral pattern approaches the planet (from above in the figure). This is consistent with the large positive torque around the time of the chosen snapshot seen in Fig. 3. The outer gap edge for $Q_o = 2.0$ is not as disrupted and this results in no secular increase in r_p for the simulated time for $Q_o = 2.0$.

In Fig. 4, large-scale spirals can still be seen for $Q_o = 1.5$. Weak fragmentation occurs without a collapse into clumps. Like $Q_o = 1.7$, the gap is unclean with significant disruption to the outer gap edge. It is no longer a clear feature as for $Q_o = 2.0$.

The surface density plots (Fig. 4), together with the torque plot (Fig. 3), show that edge modes significantly modify torques from those expected for standard type II migration. Specifically for our models, edge modes are associated with the outer gap edge and lead to a secular increase in orbital radius (Fig. 2). We shall see below that this is because edge modes provide overdensities inside the gap, despite the tendency for giant planets to clear the gap of material.

4.2 Gap evolution

In this section we use the following prescription to examine the evolution of the gap structure. We first calculate the azimuthally averaged relative surface density perturbation,

$$\delta\Sigma(r) = \left\langle \frac{\Sigma - \Sigma(t=0)}{\Sigma(t=0)} \right\rangle_\phi . \tag{7}$$

We define the *outer gap edge* as $r_{e,out} > r_p$ such that $\delta\Sigma(r_{e,out}) = 0$, and similarly for the *inner gap edge* $r_{e,in} < r_p$. The *outer gap depth* is defined as $\delta\Sigma$ averaged over $r \in [r_p, r_{e,out}]$. We also define the *outer gap width*, in units of the Hill radius, as $w_{out} = |r_{e,out} - r_p|/r_h$ and the *inner gap width* as $w_{in} = |r_{e,in} - r_p|/r_h$. The *gap asymmetry* is $w_{out} - w_{in}$. Running-time-averaged plots of these quantities are shown in Fig. 5.

Edge modes have a gap-filling effect. The case $Q_o = 1.5$, for which the planet immediately migrates outwards, has the smallest magnitude of gap depth throughout. The $Q_o = 2.0$ case has the deepest gap and is non-migrating over the simulation time-scale. In the $Q_o = 1.7$ case, the magnitude of gap depth decreases relative to that for $Q_o = 2.0$ after about $t = 80P_0$. Note that this corresponds to outward migration for $Q_o = 1.7$. These observations suggest that material brought into the gap by edge modes is responsible for outward migration.

We have defined gap asymmetry as the distance from the planet to the outer gap edge minus the distance between the planet and the inner gap edge. It follows that the more negative the gap asymmetry is, the closer the planet is to the outer gap edge. Fig. 5 shows the planet is located closer to the outer gap edge in discs with lower Q_o than in discs with higher Q_o. Furthermore, the non-migrating $Q_o = 2.0$ case reaches a constant asymmetry, whereas in the outwards-migrating cases asymmetry decreases with time.

Recall that edge mode spiral arms are associated with the outer gap edge. The trend above suggests that the planet is moving outer gap edge material inwards via horseshoe turns (this would also be consistent with shallower gaps with decreasing Q_o.). This provides a

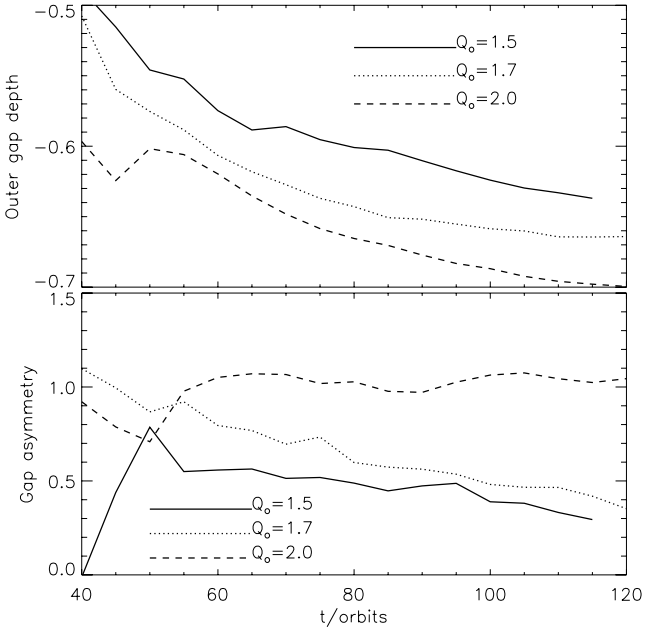

Figure 5. Running-time averages of gap properties: the dimensionless outer gap depth (top) and the gap asymmetry in units of Hill radius (bottom). These quantities are defined in Section 4.2.

positive torque on the planet. If on average this effect dominates over sources of negative torques, e.g. Lindblad torques or coincidence of an edge mode spiral arm with the outer planetary wake (Lin & Papaloizou 2011a), then the planet should on average migrate outwards, i.e. closer to the outer gap edge.

5 A FIDUCIAL CASE

In order to understand the mechanism by which edge mode spiral arms lead to outward migration, we here focus on the case $Q_o = 1.7$. This simulation has been extended to $t = 140P_0$. Figs 6 and 7 summarize this simulation in terms of the evolution of the planet's orbit and the disc's surface density perturbation. The orbit remains fairly circular ($e < 0.06$) with no overall change in eccentricity. However, the semi-major axis a increases more noticeably than the orbital radius r_p.

In Fig. 6, a rapidly increases towards the end of the simulation ($t > 130P_0$). This is because edge modes eventually caused the

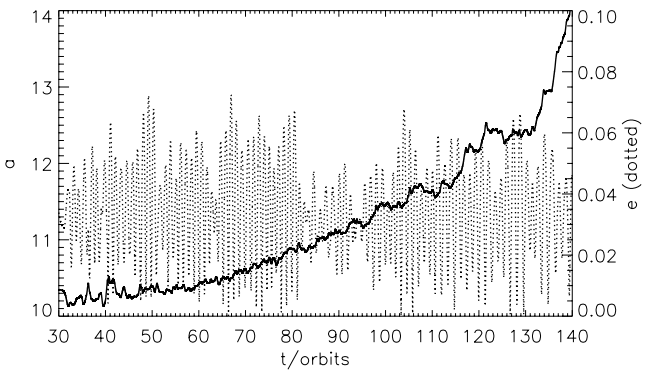

Figure 6. Orbital evolution of the planet in the $Q_o = 1.7$ disc, in terms of Keplerian semi-major axis a (solid) and eccentricity e (dotted). These have been calculated assuming Keplerian ellipses without accounting for the disc potential.

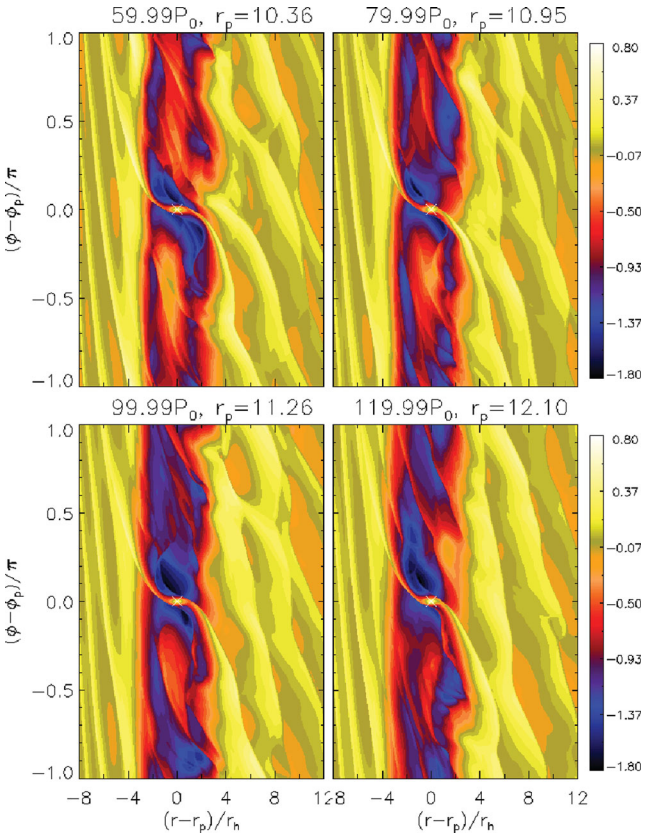

Figure 7. Overall evolution of the $Q_o = 1.7$ case. The logarithmic relative surface density perturbation $\log[\Sigma/\Sigma(t=0)]$ is shown.

planet to move into the disc lying beyond the original outer gap edge. The planet effectively leaves the gap. At this point, we found the surface density contrast ahead and behind the planet conforms to outward type III migration (Masset & Papaloizou 2003; Pepliński, Artymowicz & Mellema 2008b). This may have resulted from the fact that edge modes in our discs supply overdensities ahead of the planet (see below), providing the initial condition, or kick, for outward runaway migration.

Once the planet is in type III migration, edge modes become irrelevant. This situation differs from migration sustained by edge mode spirals associated with the gap edge, where the planet can still be seen to reside in an annular gap. Henceforth, we shall focus on the time frame in which this configuration holds ($t \lesssim 130P_0$).

Fig. 7 shows the outer disc ($r > r_p$) is more unstable than the inner disc ($r < r_p$). Large-scale, coherent spirals are maintained throughout the simulation. The gap is unclean with material brought into it by the edge modes. Overdensities may lie within the planet's co-orbital region ($2.5r_h \gtrsim r - r_p > 0$). Such material is expected to execute inward horseshoe turns and exert a positive torque on the planet.

The above effect causes the planet to move outwards, towards the outer gap edge where the surface density is higher. The planet can then interact with that material by moving it through inward horseshoe turns, providing further positive torque. The torque magnitude should also increase with the migration speed. These effects can result in a positive feedback akin to that seen in classic type III migration (Masset & Papaloizou 2003), which is consistent with the faster-than-linear increase in a for $t < 130P_0$.

This interaction is local and depends primarily on the surface density, so the background Toomre Q parameter, which decreases

with radius on a global scale, is not expected to be of direct relevance in this feedback mechanism apart from its dependence on the surface density.

5.1 Surface density asymmetry

In Fig. 8 we plot two interaction events between an edge mode spiral arm and the planet. In the first, we see that the spiral wave disturbance extends into within $2r_{\rm h}$ upstream of the planet. This causes a surface density asymmetry ahead and behind the planet, the configuration here corresponding to positive co-orbital torque. This is more apparent in the second event: overdensity builds up just ahead of the planet as material undergoes inward horseshoe turns. The fluid shocks while executing the U-turn, since giant planets induce shocks close to their orbital radii (Lin & Papaloizou 2010). A stable gap would have been cleared of material by a Jovian mass planet and such an overdensity ahead of the planet would not exist.

It is important to note that we have chosen the snapshots in Fig. 8, where the orbital radius $r_{\rm p}$ increases, to demonstrate how edge modes can provide a positive torque. However, not every passage of the spiral arm increases $r_{\rm p}$, as implied by the non-monotonic migration. An example is shown in Fig. 9. Since the outer planetary wake is associated with negative Lindblad torques, surface density perturbations due to edge modes may enhance it when the two overlap.

The overall outward migration implies positive torques produced by edge modes are on average more significant. This may not be surprising since the positive torque comes from material crossing $r_{\rm p}$. This is also the mechanism for type III migration (Masset & Papaloizou 2003) which can be much faster than migration due to Lindblad torques.

5.2 Torques and mode amplitudes

To emphasize the significance of edge modes on disc–planet torques we can compare the fiducial case $Q_{\rm o} = 1.7$ to the non-migrating case $Q_{\rm o} = 2.0$. Fig. 10 shows the time-averaged evolution of non-axisymmetric modes in the outer disc ($r > r_{\rm p}$) and torques in these two cases. The amplitude of the $m^{\rm th}$ Fourier mode is defined as $|C_m/C_0|$, where

$$C_m = \int_{r_{\rm p}}^{r_{\rm o}} {\rm d}r \int_0^{2\pi} {\rm d}\phi \Sigma(r,\phi) \exp(-{\rm i}m\phi), \tag{8}$$

and we plot $|C_m/C_0|$ for $m = 2, 3$.

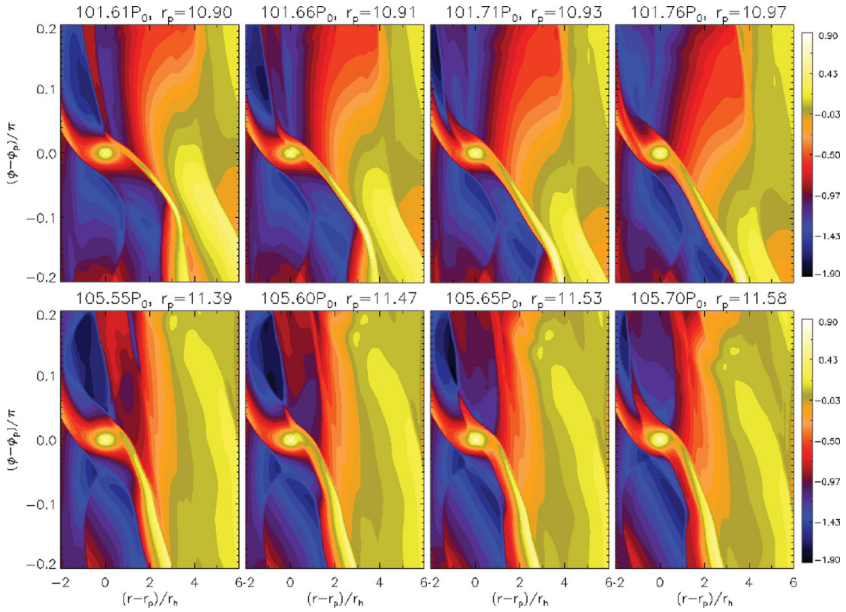

Figure 8. Two examples of how the passage of an edge mode spiral arm by the planet can increase its orbital radius. The disc model is $Q_{\rm o} = 1.7$ and the logarithmic relative surface density perturbation $\log[\Sigma/\Sigma(t=0)]$ is shown.

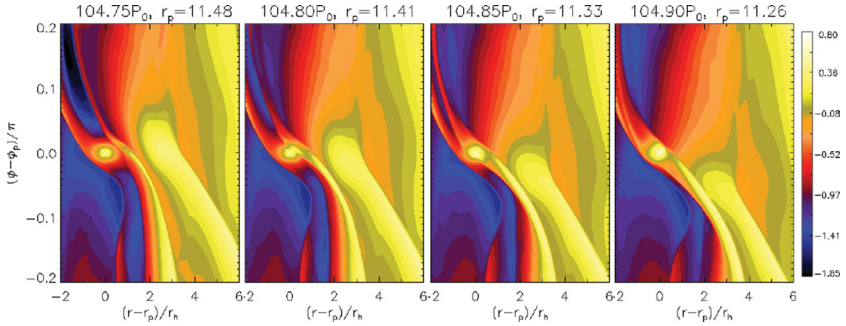

Figure 9. Passage of an edge mode spiral arm by the planet in the $Q_{\rm o} = 1.7$ disc model. The logarithmic relative surface density perturbation $\log[\Sigma/\Sigma(t=0)]$ is shown. In this event the orbital radius decreases because the planetary wake is effectively enhanced by the edge mode. Nevertheless, like Fig. 8, this plot also demonstrates how edge modes can contribute positively to the torque by supplying material into the co-orbital region for the planet to scatter inwards.

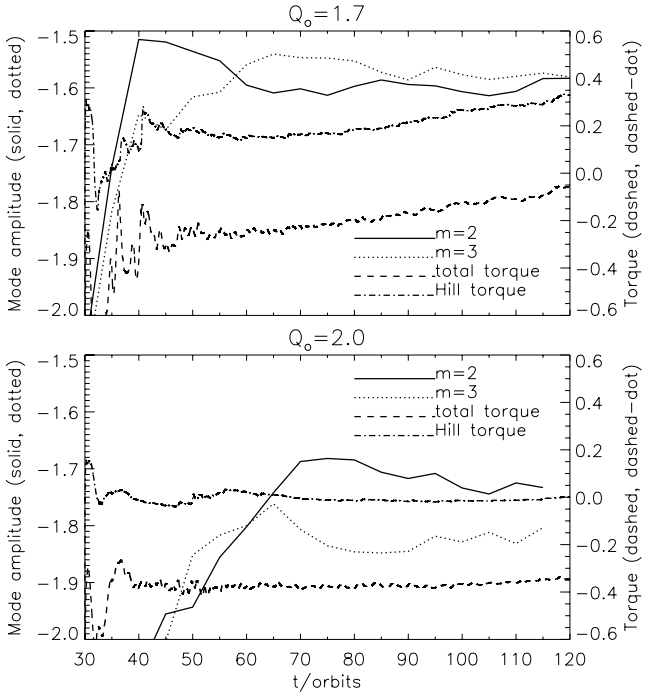

Figure 10. Evolution of the amplitude of the $m = 2$ (solid) and $m = 3$ (dotted) modes in surface density in the outer disc $r \in [r_p, r_o]$ in comparison to the total disc-on-planet torque (dashed) and the torque contribution from the Hill sphere (dash–dotted). All quantities are running-time averages. Fourier modes have been normalized by the axisymmetric amplitude and are plotted on a logarithmic scale. The upper plot is $Q_o = 1.7$, in which the planet migrates outwards. The lower plot is the non-migrating $Q_o = 2.0$ case.

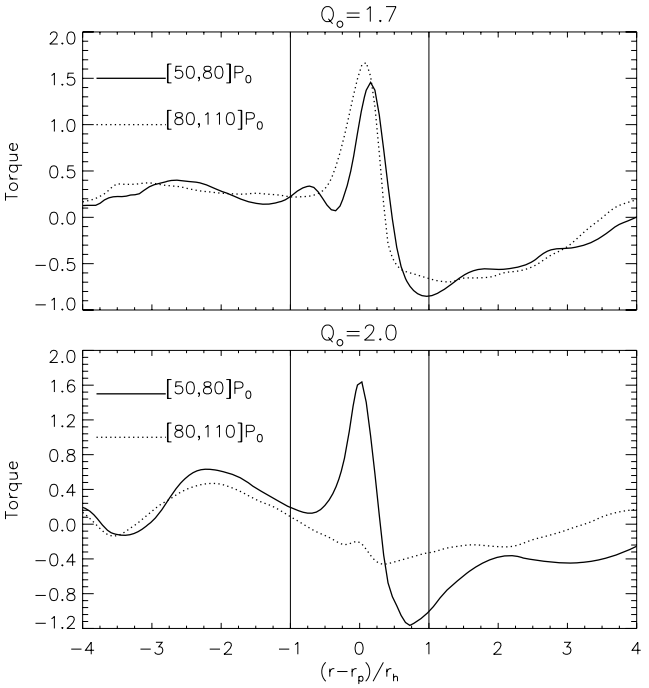

Figure 11. Torque densities averaged over $t \in [50, 80]P_0$ (solid) and over $t \in [80, 110]P_0$ (dotted). The upper plots are from the $Q_o = 1.7$ case, which display outward migration and the lower plots are from the non-migrating $Q_o = 2.0$ case. Vertical lines in each plot indicate the Hill radius.

The modes have larger amplitudes for $Q_o = 1.7$ and the total torque increases with time.[2] The figure shows that this is attributed to torques from within the Hill radius. By contrast, although the $Q_o = 2.0$ case also develops large-scale spirals later on, they are of smaller amplitude and do not make the Hill torque positive. The total time-averaged torque remains fairly constant.

Fig. 10, along with Figs 7–9, confirms that large-scale spirals which extend into the gap can provide significant torques. Edge modes naturally fit this description since they are associated with vortensity maxima just inside the gap. Because the outer disc is more unstable, the corotation radius r_c of edge modes lies beyond r_p so its pattern speed is smaller than the planet's rotation. Thus, overdensities associated with corotation approach the planet from upstream, but because r_c is actually within the planet's co-orbital region, the associated fluid elements are expected to execute inward horseshoe turns upon approaching the planet. This provides a positive torque on the planet, and if the edge mode amplitude is large enough, it may reverse the usual tendency for inward migration.

The picture outlined above is consistent with the fact that edge modes have corotation at vortensity maxima. A giant planet can induce shocks very close to its orbital radius and vortensity is generated as fluid particles execute horseshoe turns across the shock. That is, vortensity maxima are associated with fluid on horseshoe orbits. So when non-axisymmetric disturbances associated with vortensity rings develop (i.e. edge modes), the associated overdensities can be expected to execute horseshoe turns.

[2] The total torque values are negative, despite overall outward migration, because the running-time average is plotted. This average includes the phase of planet release, when the disc–planet torque is large and negative.

5.3 Torque distribution

The analysis above suggests that torques from within the gap are responsible for the gradual increase in r_p or a. Fig. 11 compares torque densities in the fiducial case to the non-migrating case. The torques have been averaged over $30P_0$ at two time intervals.

For $t \in [50, 80]P_0$ radial plots for both cases show a positive torque at r_p. By $t \in [80, 110]P_0$ this torque has diminished for $Q_o = 2.0$. This is expected for Jovian planets as they open a clean gap leaving little material near r_p to torque the planet. However, for $Q_o = 1.7$, this torque is maintained (and even slightly increased) by the edge modes because they bring material into the co-orbital region. Note that the planet in the $Q_o = 1.7$ case is migrating outwards for $t \in [80, 110]P_0$, so migration itself may also contribute to sustaining the torque.

This torque is caused by overdensity ahead in comparison to that behind the planet, i.e. material flowing radially inwards across the planet's orbital radius, as can be seen in Fig. 8. However, unlike the single scattering events by vortices or spirals described in Lin & Papaloizou (2010, 2011a), which dominate most of the migration, here one has to average over many spiral–planet interaction events to see the migration.

6 SUMMARY AND DISCUSSION

We have performed self-gravitating disc–planet simulations to see the effect of large-scale spiral modes associated with a gap opened by a giant planet on its migration. In our disc models, edge modes lead to outward migration over time-scales of a few tens of initial orbital periods. This contrasts to standard type II inwards migration

on viscous time-scales (Lin & Papaloizou 1986). This difference demonstrates that gap instabilities significantly affect planetary migration in massive discs.

It is important to note that we have specifically considered unstable planetary gaps. This differs from disc models employed by Baruteau et al. (2011) and Michael et al. (2011), which are at least twice as massive as our fiducial case and develop gravitational instabilities without a planet. Furthermore, the planet does not open a gap in their models. By contrast, gravitational activity in our discs is entirely due to the planet opening a gap. The instability then back reacts on planet migration.

Baruteau et al. (2011) argued that a single giant planet in a massive, gravito-turbulent disc effectively undergoes type I migration, which resulted in rapid inwards migration in their models. This again contrasts to our less massive discs, which are not gravito-turbulent and the interaction we consider is that between a planet and large-scale spiral waves associated with gap edges.

In the planet's frame, an edge mode spiral, with corotation at a vortensity maximum exterior to $r_{\rm p}$, approaches the planet from $\phi > \phi_{\rm p}$. However, the disturbance extends into the planet's co-orbital region, so there are associated overdensities that execute inward horseshoe turns, which provide a positive torque. The resulting outward migration means that this positive torque must on average exceed any negative torques.

In order to sustain this positive torque, edge modes need to be sustained to supply material to the planet for interaction. This in turn requires the existence of vortensity maxima, despite the development of edge modes destroying them. However, they are easily regenerated by giant planets because they induce shocks which act as a source of vortensity (Lin & Papaloizou 2010).

Planetary migration observed here closely resembles classic type III migration because it relies on torques from the co-orbital region and the accelerated increase in semi-major axis indicates a positive feedback (Masset & Papaloizou 2003; Pepliński et al. 2008b). Accelerated migration may be expected because edge modes move the planet toward regions of higher surface density (the gap edges) so more material enters the planet's co-orbital region. However, other outcomes are also conceivable (see Section 6.3).

The main difference from the type III migration originally described by Masset & Papaloizou is that the flow across the planet's orbit is non-smooth, because edge modes provide distinct fluid blobs, rather than a continuous flow across $r_{\rm p}$. Our results above may be interpreted as a discontinuous runaway type III migration.

Also, where type III migration usually applies to partial gaps and therefore Saturn-mass planets, the Jovian mass planet used here resides in a much deeper gap. Radial mass flux across the gap is still possible, despite the gap-opening effect of Jovian planets, because the unstable edge modes protrude the gap edge.

Our understanding of the effect of edge modes is based on the geometry of the gap structure. That is, the existence of a vortensity maximum (equivalently Q-maximum) close to the gap edge, and its association with global spiral modes. Thus the mechanism we have identified, that edge modes bring material to the planet for interaction, should be a robust phenomenon for planetary gaps in massive discs.

6.1 Comparison to previous work

Migration here differs to scattering by an edge mode spiral arm described by Lin & Papaloizou (2011a), in which a single interaction increases the orbital radius of a Saturn mass planet by 40 per cent over a time-scale of only $4P_0$, moving it out of its gap (see their fig. 20). By contrast, the 2 Jupiter mass planet simulated here migrates outwards by 20 per cent over a few tens of P_0, during most of which it remains in a gap, and there are multiple encounters with edge mode spiral arms.

In both cases the torque comes from material crossing the planet's orbital radius, but interaction occurs more readily with the less massive Saturn mass planet since its gap-opening effect is weaker. Furthermore, the EOS employed in the preliminary simulation of Lin & Papaloizou (2011a) allows high surface densities near the planet, potentially increasing the co-orbital torque magnitudes.

Note that if the planet is first allowed to move after edge modes develop, then the initial migration direction would depend on the relative position of the edge mode spiral with respect to the planet. This was the case in Lin & Papaloizou (2011a), the planet being released when a spiral arm is just upstream.

However, for the models discussed in this paper, edge modes do not develop before planet release ($t = 30P_0$). This can be seen by the well-defined max(Q), equivalently vortensity maximum, in the gap profiles in Fig. 1. The onset of edge modes would have destroyed this local maximum (Lin & Papaloizou 2011a, fig. 14).

6.2 Implications

A consequence of the above is that formation of a clean gap is expected to become increasingly difficult in massive discs. Planetary gaps correspond to the existence of vortensity maxima, but these become unstable to edge modes in massive discs and instability tends to fill the gap. Therefore, the standard picture and formulae for type II migration should not be applied to gap opening planets in massive protoplanetary discs.

We remark that migration is not only relevant to planets in protoplanetary discs. Analogous interactions have been discussed in the context of stars in black hole accretion discs (Kocsis, Yunes & Loeb 2011; McKernan et al. 2011). Self-gravity could be important in outer regions of these discs, so our results may also be relevant to these situations.

6.3 Outstanding issues

Our focus in this paper was to identify the mechanism by which edge modes may torque up the planet. We have thus considered one particular disc model and only varied one parameter, the surface density scale. Although the simulation time-scales were sufficient for our purpose, these are short compared to disc lifetimes.

We expect inter-dependencies between planet, disc properties and migration for the specific situation of a planet interacting with a gravitationally unstable gap, which was induced by it in the first place. In our fiducial simulation the planet eventually goes into classic type III migration. However, if the planet moves out and leaves its gap with a slow enough migration speed, it may open a new gap which develops edge modes[3] and induces further outward migration, or even fragmentation (Section 3). It is also conceivable for some disc parameters, the positive torque from edge modes are sufficiently small, so that it may be balanced by inwards type II migration on longer time-scales. Possible long-term outcomes need to be explored in a parameter study.

[3] Edge modes also require the existence of a wider disc beyond the gap edge, so outward migration should become ineffective once the planet moves close the disc outer boundary.

It should be noted that our adopted disc model is biased towards outward migration because the Toomre Q decreases outwards (approximately like $r^{-1/2}$) so edge modes associated with the outer disc develop preferentially. This is consistent with the expectation that typical discs become more self-gravitating with increasing radius. However, if the disc model was such that the inner disc is more unstable, then edge modes should promote inward migration. Moreover, if independent edge modes of comparable amplitude develop on either side of the gap there could be little migration overall.

Significant torques originate from material close to the planet, so numerical treatment of the Hill sphere is a potential issue. This concern also applies to standard type III migration, but we remark that the adopted EOS was originally designed for numerical studies of type III migration (Pepliński et al. 2008a). Furthermore, the fully self-gravitating discs considered here are what is required for accurate simulations of type III migration (Crida et al. 2009). As a check we have also performed lower resolution simulations which also resulted in outward migration.

This EOS mimics heating near the planet but is not a quantitative model for the true thermodynamics. If this EOS underestimates the heating, then the positive torque could be overestimated and vice versa. On the other hand, edge mode corotation resides outside the Hill radius but still inside the gap. Thus, the numerical treatment within the Hill radius does not affect the existence of edge modes and their associated overdensities should affect torques originating from the co-orbital region in the way described in this paper.

ACKNOWLEDGMENTS

M-KL acknowledges support from St John's College, Cambridge, the Isaac Newton Trust and an Overseas Research Award.

REFERENCES

Armitage P. J., Hansen B. M. S., 1999, Nat, 402, 633
Artymowicz P., 2004, KITP Conference: Planet Formation: Terrestrial and Extra Solar Migration Type III
Ayliffe B. A., Bate M. R., 2010, MNRAS, 408, 876
Baruteau C., Masset F., 2008, ApJ, 678, 483
Baruteau C., Meru F., Paardekooper S.-J., 2011, MNRAS, 416, 1971
Crida A., Baruteau C., Kley W., Masset F., 2009, A&A, 502, 679
Durisen R. H., Boss A. P., Mayer L., Nelson A. F., Quinn T., Rice W. K. M., 2007, in Reipurth B., Jewitt D., Keil K., eds, Protostars and Planets V. Univ. Arizona Press, Tucson, p. 607
Godon P., 1996, MNRAS, 282, 1107
Goldreich P., Tremaine S., 1979, ApJ, 233, 857
Goldreich P., Tremaine S., 1980, ApJ, 241, 425
Kocsis B., Yunes N., Loeb A., 2011, Phys. Rev. D, 84, 024032
Lin D. N. C., Papaloizou J., 1986, ApJ, 309, 846
Lin M.-K., Papaloizou J. C. B., 2010, MNRAS, 405, 1473
Lin M.-K., Papaloizou J. C. B., 2011a, MNRAS, 415, 1445
Lin M.-K., Papaloizou J. C. B., 2011b, MNRAS, 415, 1426
Lovelace R. V. E., Li H., Colgate S. A., Nelson A. F., 1999, ApJ, 513, 805
Lufkin G., Quinn T., Wadsley J., Stadel J., Governato F., 2004, MNRAS, 347, 421
McKernan B., Ford K. E. S., Lyra W., Perets H. B., Winter L. M., Yaqoob T., 2011, MNRAS, 417, L103
Masset F., 2000a, A&AS, 141, 165
Masset F. S., 2000b, in Garzón G., Eiroa C., de Winter D., Mahoney T. J., eds, ASP Conf. Ser. Vol. 219, Disks, Planetesimals, and Planets. Astron. Soc. Pac., San Francisco, p. 75
Masset F. S., Papaloizou J. C. B., 2003, ApJ, 588, 494
Meschiari S., Laughlin G., 2008, ApJ, 679, L135
Michael S., Durisen R. H., Boley A. C., 2011, ApJ, 737, L42
Nelson A. F., Benz W., 2003a, ApJ, 589, 556
Nelson A. F., Benz W., 2003b, ApJ, 589, 578
Paardekooper S.-J., Papaloizou J. C. B., 2009, MNRAS, 394, 2297
Papaloizou J. C. B., Lin D. N. C., 1989, ApJ, 344, 645
Papaloizou J. C., Savonije G. J., 1991, MNRAS, 248, 353
Pepliński A., Artymowicz P., Mellema G., 2008a, MNRAS, 386, 164
Pepliński A., Artymowicz P., Mellema G., 2008b, MNRAS, 387, 1063
Pierens A., Huré J.-M., 2005, A&A, 433, L37
Sellwood J. A., Kahn F. D., 1991, MNRAS, 250, 278
Toomre A., 1964, ApJ, 139, 1217
Zhang H., Yuan C., Lin D. N. C., Yen D. C. C., 2008, ApJ, 676, 639

This paper has been typeset from a TEX/LATEX file prepared by the author.